Supplement of Atmos. Chem. Phys., 19, 9431–9451, 2019
https://doi.org/10.5194/acp-19-9431-2019-supplement

Atmospheric Chemistry and Physics
Open Access
EGU

Supplement of

A study on harmonizing total ozone assimilation with multiple sensors

Yves J. Rochon et al.

Correspondence to: Yves J. Rochon (yves.rochon@canada.ca)

The supplemental material contains three complementary tables on comparisons of OMI and ground-based total column ozone measurements, followed by five complementary figures covering different topics.

Figures S4 and S5 and the text below describe the elements of the background ozone error covariances applied with the assimilation experiments. The two figures depict the background error horizontal and vertical correlations. The resultant horizontal correlation half widths at half maximum are ~125 km near the surface and increase from ~165 km at 100 hPa to just under 750 km at 1 hPa. The vertical correlations have half width at half maximum values between 0.5 and 1 km between the top of the boundary layer and 100 hPa, and are nearly equal the model vertical resolutions above 100 hPa with values ranging from ~0.5 km at 100 hPa to ~3.5 km at 1 hPa.

The background error correlations for ozone were obtained as follows. The third order autoregressive correlation model (TOAR; Gaspari and Cohn, 1995) was applied to globally homogeneous, isotropic, and separable horizontal and vertical error correlations obtained from a spectral space representation. The initial correlations were calculated using monthly six-hour time differences of the free running GEM-LINOZ model as proxy to six-hour forecast errors (Polavarapu et al., 2005; Jackson et al., 2008; Section 5.5 in Bannister, 2008). Smoothing was applied to the vertical level-dependent set of derived error correlation half widths at half maxima of the TOAR functions.

The applied monthly background ozone error standard deviations vary with latitude and vertical level. They were obtained from a single iteration of the Desroziers et al. (2005) approach with an assimilation of the Microwave Limb Sounder (MLS) data (Waters et al., 2006; Livesey et al., 2006, 2013; Froidevaux et al., 2008) applied following originally assigned ozone background error standard deviations of 5 % in the stratosphere and upper troposphere. The resulting values at sample vertical levels of 1, 10, 50, and 300 hPa in the ranges of ~6-12 %, ~3-5 %, ~5-15 %, and ~15-24 %, respectively. Constant extrapolation in absolute value uncertainty was imposed for lower tropospheric levels with resultant percentage values being ~15-16 % of the Fortuin and Kelder (1998) climatology in volume mixing ratio.

References

Bannister, R. N.: A review of forecast error covariance statistics in atmospheric variational data assimilation. I: Characteristics and measurements of forecast error covariances, Q. J. R. Meteorol. Soc. 134, 1951–1970, https://doi.org/10.1002/qj.339, 2008.

Desroziers, G., Berre, L., Chapnik, B., and Poli, P.: Diagnosis of observation, background, and analysis-error statistics in observation space, Q. J. R. Meteorol. Soc., 131, 3385-3396, https://doi.org/10.1256/qj.05.108, 2005.

Fortuin, J. P., and Kelder, H.: An ozone climatology based on ozonesonde and satellite measurements, J. Geophys. Res., 103, 31,709-31,734, https://doi.org/10.1029/1998JD200008, 1998.

Froidevaux, L., and Coauthors: Validation of Aura Microwave Limb Sounder stratospheric ozone measurements, J. Geophys. Res., 113, D15S20, https://doi.org/10.1029/2007JD008771, 24 pp., 2008.

Gaspari, G., and Cohn, S.: Construction of correlation functions in two and three dimensions, Q. J. R. Meteorol. Soc., 125, 723-757, https://doi.org/10.1002/qj.49712555417, 1995.

Jackson, D.R., Keil, M., and Devenish, B.J.: Use of Canadian Quick covariances in the Met Office data assimilation system, Q. J. R. Meteorol. Soc., 14, 1567-1582. https://doi.org/10.1002/qj,294, 2008.

Livesey, N. J., Van Snyder, W., Read, W. J., and Wagner, P. A.: Retrieval algorithms for the EOS Microwave Limb Sounder (MLS), IEEE Trans. Geosci. Remote Sens., 44, 1144–1155, https://doi.org/10.1109/TGRS.2006.872327, 2006.

Livesey, N. J., and Coauthors: Earth Observing System (EOS) Aura Microwave Limb Sounder (MLS): Version 3.3 and 3.4 Level 2 data quality and description document, JPL D-33509, Version 3.3x/3.4x-1.1, Jet Propulsion Laboratory, 158 pp., May 14, 2013. [Available from: http://mls.jpl.nasa.gov/data/v3_data_quality_document.pdf., last access: 17 July 2019]

Polavarapu, S., Ren, S., Rochon, Y., Sankey, D., Ek, N., Koshyk, J., and Tarasick, D.: Data assimilation with the Canadian Middle Atmosphere Model, Atmos.-Ocean, 43. 77-100, https://doi.org/10.3137/ao.430105, 2005.

Waters, J. W., and Coauthors: The Earth Observing System Microwave Limb Sounder (EOS MLS) on the Aura satellite, IEEE Trans. Geosci. Remote Sens., 44, 1075–1092, https://doi.org/10.1109/TGRS.2006.873771, 2006.

Region	Station name	WMO ID[+]	Latitude (deg)	Longitude (deg)	Elevation (m)	Mean differences (%) [# of points]		
						Summer 2014	Summer 2015	Winter 2015
North America and Greenland	Alert	018	82.45	-62.51	220	0.65 [47]	-0.49 [43]	
	Edmonton	021	53.55	-114.11	752	2.34 [53]	^2.60 [103]	^1.12 [73]
	Resolute	024	74.71	-94.97	68	0.56 [36]	^0.35 [102]	
	Toronto	065	43.78	-79.47	202	0.99 [53]		
	Goose Bay	076	53.31	-60.36	26	^0.72 [62]	^1.94 [92]	^0.21 [63]
	Churchil	077	58.74	-94.07	26	0.81 [50]	-0.31 [95]	0.85 [52]
	Saturna Island	290	48.78	-123.13	202	1.74 [53]	^1.05 [102]	0.94 [50]
	Eureka	315	79.99	-85.93	8	-0.61 [53]	^-1.32 [104]	
	Bondville	357	40.05	-88.37	213	-0.26 [8]	0.67 [46]	-0.52 [25]
	Boulder	424	40.13	-105.24	1689	^0.18 [150]	^1.41 [137]	-0.20 [96]
	Raleigh	461	35.73	-78.68	272	^4.34 [4]	3.14 [46]	0.79 [32]
	Fort Peck	362	48.31	-105.10	634		3.50 [46]	1.97 [37]
	Houston	484	29.72	-95.34	64		0.12 [49]	-1.23 [27]
	Rocky Mountain	392	40.03	-105.53	2923	2.14 [53]	*4.03 [44]	-1.93 [35]
	Sondrestrom	267	67.00	-50.62	300	-1.42 [51]	-1.38 [55]	-2.38 [2]
Europe and Africa	Uccle	053	50.80	4.35	100	^-0.87 [134]		
	Hradec Kralove	096	50.18	15.84	285	^-0.87 [106]	^-1.21 [81]	-0.17 [28]
	Hohenpeissenberg	099	47.81	11.01	975	0.59 [47]	0.53 [50]	0.91 [40]
	Oslo	165	59.94	10.72	90	-0.93 [54]	-1.28 [48]	-1.72 [10]
	Norrkoeping	279	58.58	16.15	43	-2.40 [56]	-2.35 [28]	-0.40 [15]
	Vindeln	284	64.24	19.77	225	-0.22 [49]	1.08 [24]	-0.13 [7]
	Valentia Observatory	318	51.93	-10.25	14	^1.72 [103]	1.88 [49]	0.94 [35]
	Poprad-Ganovce	331	49.03	20.32	706	-0.99 [42]	-0.42 [52]	-0.44 [29]
	Thessaloniki	261	40.52	22.97	50	-0.49 [45]	-0.58 [48]	-1.85 [24]
	Kislovodsk	282	43.73	42.66	2070	2.79 [48]	2.42 [42]	-1.03 [44]
	Rome	305	41.90	12.50	75	-0.23 [55]	0.33 [44]	0.77 [38]
	Obninsk	307	55.10	36.61	100	-1.07 [57]	-1.09 [52]	-0.76 [14]
	De Bilt	316	52.10	5.18	24	-2.29 [54]	-1.39 [48]	-2.49 [31]
	Reading	353	51.44	-0.94	66	^2.14 [112]	0.43 [46]	0.85 [33]
	Andoya	476	69.28	16.01	380	-1.03 [22]	-1.50 [33]	
	Murcia	346	38.00	-1.16	69	-0.07 [54]		
	Manchester	352	53.47	-2.23	76	-0.65 [47]	-0.47 [51]	-1.78 [19]
	La Coruña	405	43.33	-8.41	65	*-4.95 [25]		
	Zaragoza	411	41.63	-0.88	258	-0.37 [53]		
	Aosta	479	45.74	7.36	570	^-0.73 [101]	-0.99 [46]	-1.24 [42]
	Tamanrasset	002	22.78	5.52	1384	-1.84 [54]		-0.71 [45]
	Marsa Matrüh	376	31.33	27.22	35	-2.41 [53]		
East Asia	Petaling Jaya	322	3.10	101.65	86	^1.58 [82]		1.18 [45]
	Pohang	332	36.03	129.38	6	-0.66 [25]		
	Minamitorishin	030	24.29	153.98	9	-0.73 [55]	-1.29 [47]	-0.40 [40]
	Mt. Waliguan	295	36.29	100.90	3810		*7.36 [42]	*-4.06 [21]
	Linan	325	30.18	119.44	132		-1.87 [32]	*-5.38 [26]
	Longfengshan	326	44.73	127.59	334		*4.15 [48]	*-21.47 [40]
	Lhasa	349	29.67	91.13	3650		*10.59 [48]	1.48 [41]
	Songkhla	345	7.20	100.60	12		-0.99 [30]	-1.24 [37]
	Bangna Bangkok	216	13.67	100.62	60			-2.20 [43]
	Anmyeon-do	513	36.54	126.33	57	-0.87 [45]		
Other	Mauna Loa	031	19.54	-155.58	3397	3.10 [53]	*4.99 [47]	^*5.08 [84]
	Paramaribo	435	5.81	-55.22	16	-0.45 [52]	0.08 [39]	0.84 [36]
	Zhongshan	478	-69.37	-76.38	11			*-5.68 [51]
	Amundsen-Scott	111	-90.00	70.24	3507			-2.17 [55]
	Marambio	233	-64.23	-56.62	198	*-5.45 [13]		0.67 [46]
	Punta Arenas	473	-53.14	-70.85	0	*-4.01 [42]	0.14[38]	0.17 [55]

[+]World Meterological Organization station identification number, ^Multiple instruments

*Identifies stations with outlier mean differences as either larger in size than 6 % or exceeding two standard deviations of the mean difference variability standard deviation over all remaining stations.

Table S1. List of time mean differences of total column ozone between OMI-TOMS and Brewer stations over July-August 2014/2015 and January-February 2015. The Bandung station, Indonesia, is not included as it was later found to have been assigned incorrect coordinates.

Region	Station name	WMO ID[+]	Latitude (deg)	Longitude (deg)	Elevation (m)	Mean differences (%) [# of points]		
						Summer 2014	Summer 2015	Winter 2015
North America and Greenland	Caribou	020	46.87	68.03	192		1.32 [11]	
	Boulder	067	40.01	-105.25	1689	-0.22 [35]	-1.03 [25]	-0.25 [19]
	Wallops	107	37.93	-75.48	13	0.26 [18]		
	Mexico City	192	19.33	-99.18	2268		*-7.57 [10]	*-4.67 [14]
	Barrow	199	71.32	-156.61	11	-1.02 [13]	-1.16 [16]	
	La Habana	311	23.14	-82.34	50	-1.43 [27]	-0.86 [5]	0.26 [12]
	Hanford	341	36.32	-119.63	73	-0.25 [32]		0.72 [22]
Europe and Africa	Tamanrasset	002	22.78	5.52	1382	-2.12 [53]	-1.82 [49]	-0.19 [46]
	Haute Provence	040	43.93	5.70	684	1.29 [27]	1.85 [47]	
	Lerwick	043	60.13	-1.18	82	0.02 [12]		
	Hradec Kralove	096	50.18	15.84	285	-0.74 [24]	-0.77 [25]	1.71 [6]
	Hohenpeissenberg	099	47.81	11.01	975	0.13 [20]	0.13 [30]	1.18 [18]
	Fairbanks	105	64.82	-147.87	138	-2.90 [14]		
	Nashville	106	36.25	-86.57	182	0.22 [41]	-1.79 [23]	0.71 [23]
	Biscarrosse	197	46.77	-100.76	511		0.56 [12]	-0.55 [13]
	Bucharest	226	44.48	26.13	100	-0.86 [11]	-0.22 [9]	0.99 [11]
	Aswan	245	23.97	32.78	190	-1.32 [10]		
	Vindeln	284	64.24	19.77	225		-1.19 [13]	
	Athens	293	37.98	23.73	280	1.55 [38]	1.64 [34]	
	Hurghada	409	27.28	33.75	7	-1.91 [50]		
	Amberd	410	40.38	44.25	2070	*6.70 [41]		
	Kyiv-Goloseyev	498	50.36	30.50	206	0.18 [27]	1.46 [51]	2.83 [18]
East Asia	Sapporo	012	43.06	141.33	26	-0.52 [25]	0.80 [13]	1.51 [11]
	Tateno	014	36.06	140.13	31	1.24 [22]	1.78 [16]	0.03 [26]
	Naha	190	26.21	127.69	28	1.18 [22]	2.72 [11]	1.12 [11]
	Xhianghe	208	39.75	116.96	29	0.01 [11]	-0.09 [5]	
	Kunming	209	25.03	102.68	1891	*-4.21 [10]		
	Bangna Bangkok	216	13.67	100.61	53	-2.43 [2]	-2.92 [2]	-2.48 [1]
Other	Mauna Loa	031	19.53	-155.58	3400	^3.16 [62]	0.75 [12]	1.92 [27]
	Buenos Aires	091	-34.58	-58.48	25	-0.37 [46]		
	Syowa	101	-69.01	39.58	22	-3.37 [2]	*-4.27 [2]	-0.13 [22]
	Amundsen-Scott	111	-89.98	-24.80	2810			-1.34 [43]
	Perith	159	-31.92	115.96	2	0.83 [19]	-0.84 [13]	-1.33 [29]
	Cachoeira	200	-22.69	-45.01	574	-2.27 [14]	-2.08 [31]	*-5.44 [28]
	Natal	219	-5.84	-35.21	49		-0.64 [26]	-1.71 [23]
	Marambio	233	-64.23	-56.62	198	-3.30 [4]		1.74 [37]
	Lauder	256	-45.04	169.68	370	0.06 [18]	-0.27 [15]	0.53 [18]
	Ushuaia	339	-54.85	-68.31	17	-1.64 [35]	-0.96 [41]	-0.83 [46]
	Comodoro	342	-45.78	-67.50	46	-0.61 [32]	-1.32 [42]	1.46 [43]
	La Quiaca	513	-22.11	-65.44	3459		-0.70 [52]	

[+] World Meterological Organization station identification number, ^Multiple instruments

*Identifies stations with outlier mean differences as either larger in size than 6 % or exceeding two standard deviations of the mean difference variability standard deviation over all remaining stations.

Table S2. List of time mean differences of total column ozone between OMI-TOMS and Dobson stations over July-August 2014/2015 and January-February 2015. The Dobson total column ozone measurements for the two summer periods were adjusted according to the bias correction as a function of the ozone effective temperature. Those for the winter period were not adjusted in the absence of the ozone effective temperature for the period. The impacts of the corrections on the mean differences for the Dobson summer periods were reductions between 0.0 and 0.4 %. The Samoa station, which is part of the WOUDC network, is not included as we had associated incorrect coordinates to it.

Region	Station name	WMO ID[+]	Latitude (deg)	Longitude (deg)	Elevation (m)	Mean differences (%) [# of points]		
						Summer 2014	Summer 2015	Winter 2015
Russia	Almaty	003	43.14	76.56	847	-0.46 [5]	-3.04 [13]	
	Vladivostok	016	43.12	131.90	138		-1.33 [4]	-2.06 [2]
	St. Pertersburg	042	59.95	30.70	74	-2.09 [6]	*-3.61 [5]	
	Bolshaya Elan	112	46.95	142.70	22		-1.60 [1]	
	Samara	115	53.25	50.22	139	1.34 [13]	2.61 [9]	
	Moscow	116	55.75	37.57	187	0.56 [4]		
	Murmansk	117	68.97	33.05	46	-1.75 [10]	-0.42 [9]	
	Nagaevo	118	59.55	150.78	115	1.00 [2]	0.78 [2]	
	Omsk	120	55.02	73.38	100	-2.24 [8]	-1.71 [7]	
	Yekaterinburg	122	56.73	61.07	300	-2.91 [2]	0.55 [7]	
	Yakutsk	123	62.02	129.72	100	-1.26 [3]	-1.04 [3]	
	Pechora	129	65.12	57.10	61	-2.47 [8]		
	Petropavko	130	53.08	158.55	78	0.62 [10]	0.83 [10]	-0.14 [5]
	Turuhansk	142	65.47	87.56	0		-2.41 [4]	
	Krasnoyars	143	56.00	92.88	277	-2.09 [1]	-1.60 [4]	
	Vitim	148	59.45	112.58	200	-1.28 [3]	-1.36 [4]	
	Hanty-Mansijsk	150	60.97	69.00	40	-0.42 [3]		
	Atiray	183	47.07	51.53	24		-0.57 [1]	
	Tiksi	186	71.58	128.90	0	2.03 [1]		
	Arkhangel'sk	271	64.55	40.58	0	-1.07 [22]	*-4.32 [14]	

[+] World Meterological Organization station identification number

Table S3. List of time mean differences of total column ozone between OMI-TOMS and filter ozonometer stations over July-August 2014/2015 and January-February 2015.

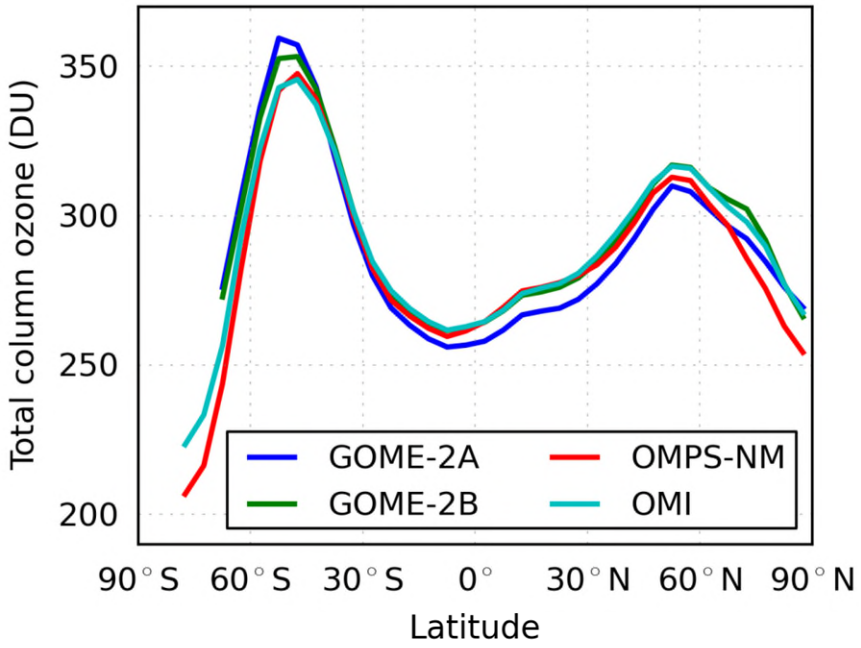

Figure S1. Total column ozone zonal means (DU) as a function of latitude (degrees), using 5° bins, for August 2014. The plot shows average latitudinal differences between instruments and allows for an approximate conversion between percentage and absolute differences.

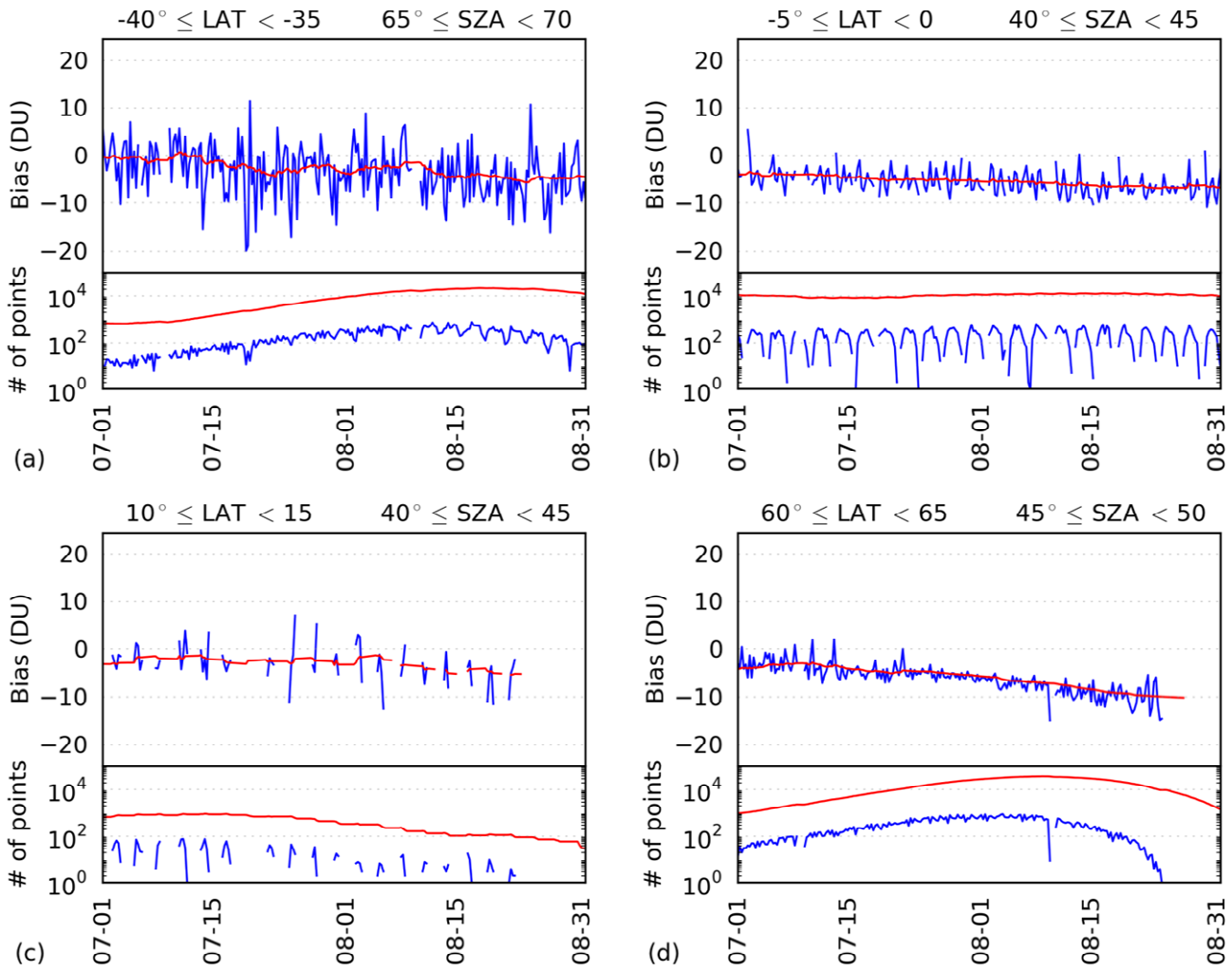

Figure S2. Time series of bias corrections (DU) for GOME-2A, corrected relative to OMI-TOMS, for July and August 2014 for selected latitude/solar zenith angle bins. Panels (a) to (d) show the bias correction for the (latitude, solar zenith angle) bins centred on (37.5°S, 67.5°), (2.5°S, 42.5°), (12.5°N, 42.5°), and (62.5°N, 47.5°), respectively, with a 5° bin width for both the latitude and solar zenith angle. In each panel, the top plot shows the biases and the bottom shows the number of points. The blue lines show individual mean differences from observations gathered in each six-hour time window from which the bias correction is derived. The red lines show the 2 week moving average bias correction. A gap in the curves denote no data availble at that time.

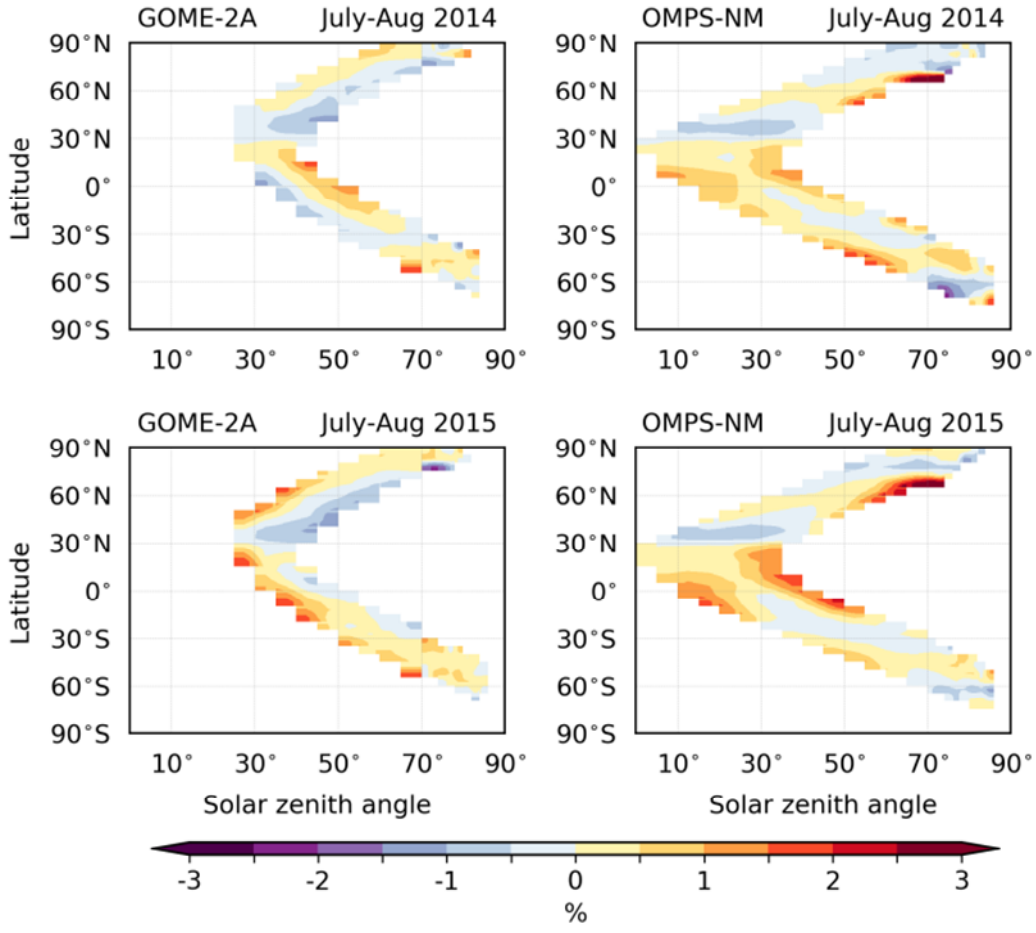

Figure S3. Residual average total column ozone differences (%) between GOME-2A, OMPS-NM and colocated OMI-TOMS data as a function of latitude (degrees) and solar zenith angle (degrees) for July-August 2014 and July-August 2015 following bias correction as a function of ozone effective temperature and solar zenith angle. The colours blue to purple denote negative differences and the colours yellow to red refer to positive differences.

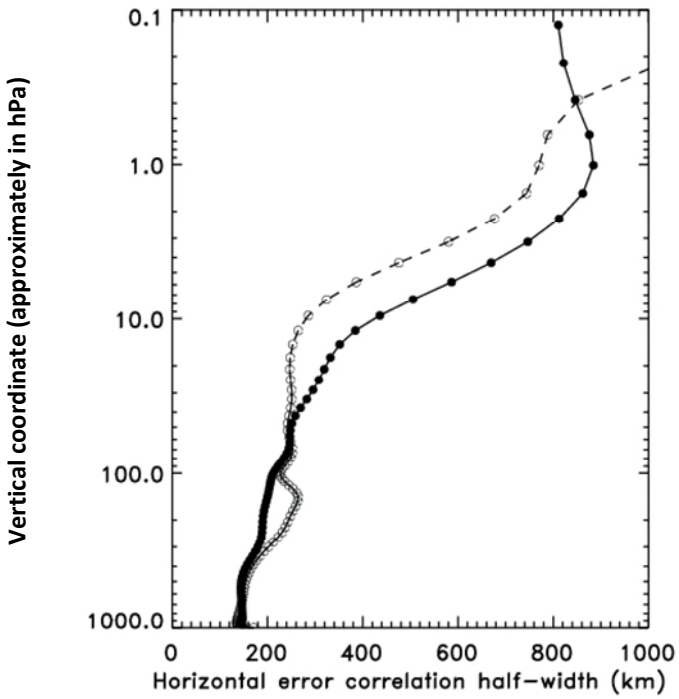

Figure S4. Half-width at half-maximum (HWHM) values for the third order autoregressive (TOAR) correlation model representing the horizontal ozone forecast error correlations derived from 48-24hr forecast differences (dashed) and 6hr time differences of the free running LINOZ ozone model (solid). The vertical axis denotes the analysis grid vertical coordinate times 1000 and can be taken as approximately equal to pressure (hPa) for a surface pressure at sea level. The shapes of the original correlation functions from these two types of differences somewhat differ.

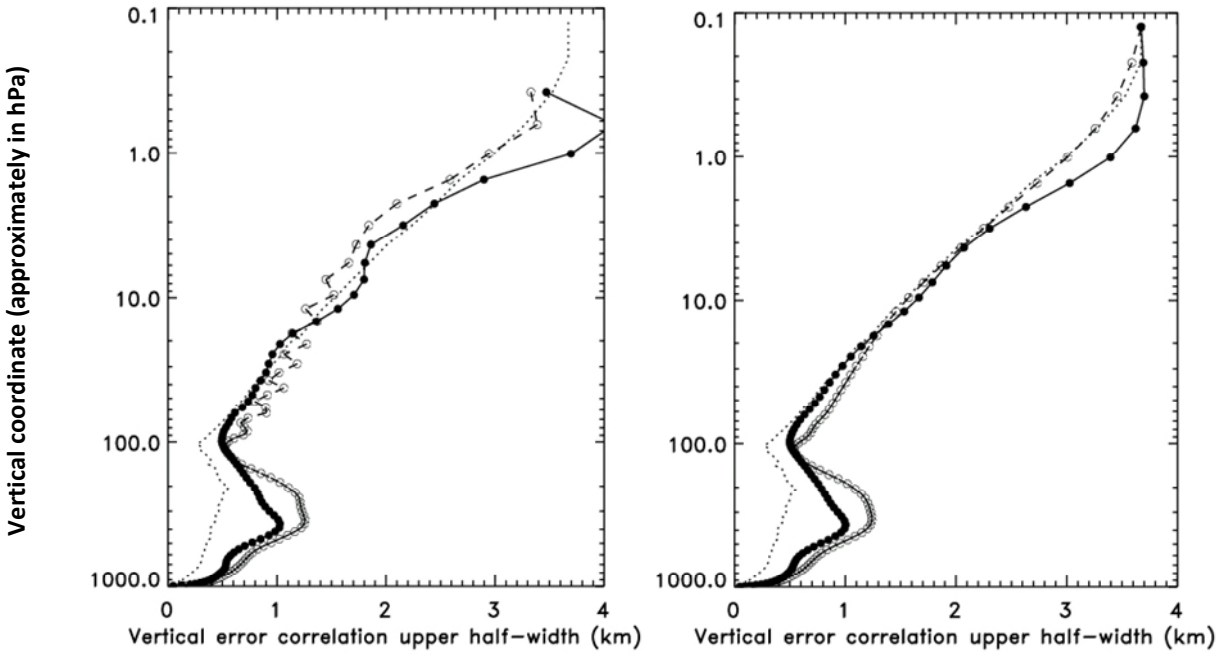

Figure S5. Upper half-width at half-maximum (HWHM) values for the third order autoregressive correlation model representing the vertical ozone forecast error correlations derived from 24-48hr forecast differences (dashed) and 6hr time differences of the free running LINOZ ozone model (solid). The dashed curve presents the approximate local vertical model resolution for the version of the model for which the correlations were derived. The vertical axis denotes the analysis grid vertical coordinate times 1000 and can be taken as approximately equal to pressure (hPa) for a surface pressure at sea level. The curves on the left panel show the initially obtained values and those on the right panel are the final values after imposing lower limits equal to separation between adjacent levels and localized vertical filtering. The vertical correlation HWHM were derived from the logarithm of the verifcal coordiantg and, for plotting purposes only, approximately converted to kilometers using the ideal gas law and an isothermal temperature of 220 Kelvin.